LET-413 is a basolateral protein required for the assembly of adherens junctions in *Caenorhabditis elegans*

Renaud Legouis*, Anne Gansmuller*, Satis Sookhareea*, Julia M. Bosher*, David L. Baillie†
and Michel Labouesse*‡

*Institut de Génétique et de Biologie Moléculaire et Cellulaire, CNRS/INSERM/ULP, BP163, 1, rue Laurent Fries, 67404 Illkirch, France
†Institute of Molecular Biology and Biochemistry, Department of Biological Sciences, Simon Fraser University, Burnaby, British Columbia, V5A 1S6 Canada
‡e-mail: lmichel@igbmc.u-strasbg.fr

Epithelial cells are polarized, with apical and basal compartments demarcated by tight and adherens junctions. Proper establishment of these subapical junctions is critical for normal development and histogenesis. We report the characterization of the gene *let-413* which has a critical role in assembling adherens junctions in *Caenorhabditis elegans*. In *let-413* mutants, adherens junctions are abnormal and mislocalized to more basolateral positions, epithelial cell polarity is affected and the actin cytoskeleton is disorganized. The LET-413 protein contains one PDZ domain and 16 leucine-rich repeats with high homology to proteins known to interact with small GTPases. Strikingly, LET-413 localizes to the basolateral membrane. We suggest that LET-413 acts as an adaptor protein involved in polarizing protein trafficking in epithelial cells.

Epithelial cells perform numerous specialized functions which rely on their pronounced apico-basal polarity. The polarized phenotype of epithelial cells is manifested by the differential sorting of plasma membrane proteins to apical and basolateral compartments and by polarization of the cytoskeleton[1]. Adherens junctions ensure adhesion between adjacent cells, whereas tight junctions (in vertebrates) or septate junctions (the presumed equivalent structure in invertebrates) maintain the separation between the apical and basolateral domains. Despite the key role of these junctions in promoting the epithelial phenotype, their biogenesis is just beginning to be analysed.

Genetic analysis in *Drosophila* has suggested that a network of scaffolding proteins organizes the apical domain of epithelial cells by interacting with different transmembrane and membrane-associated proteins to allow the assembly of specialized junctions[2–7]. The transmembrane protein Crumbs, and the membrane-associated proteins Discs-large (DLG) and Discs-lost (DLT) have attracted particular attention in this process[3,5,8]. DLG, the founding member of the MAGUK family, and DLT contain PDZ domains, which mediate protein–protein interactions and have been implicated in the clustering of membrane proteins to specific subcellular regions in various cell types[3,5,9]. For instance, DLT can interact with itself and with Crumbs[5,6]. In *crumbs*, *dlt* and *dlg* mutants, epithelial cell polarity is lost and junctions are not assembled[3,6,8]. Elegant studies in *C. elegans* have shown that basolateral proteins can also depend on PDZ proteins for their proper localization to basolateral membranes. In animals mutant for the PDZ proteins LIN-2, LIN-7 or LIN-10, the epidermal growth factor (EGF) receptor protein LET-23 is not localized to the basolateral membrane; as a consequence the signalling process involved in vulval induction is defective and animals become vulvaless[10–12].

We are using the *C. elegans* embryo as a model to investigate how cell polarity is established. Although the precise molecular composition of epithelial junctions in *C. elegans* has yet to be determined, a complex of cadherin, α-catenin and β-catenin, encoded by the genes *hmr-1*, *hmp-1* and *hmp-2* respectively, was shown to co-localize with adherens junctions[13]. Inactivation of this complex does not affect cell adhesion or apico-basal polarity, but disrupts the anchorage of actin filaments during two morphogenetic events involving epidermal cells, namely ventral enclosure and elongation[13]. Ventral enclosure is a process similar to epiboly, during which two lateral
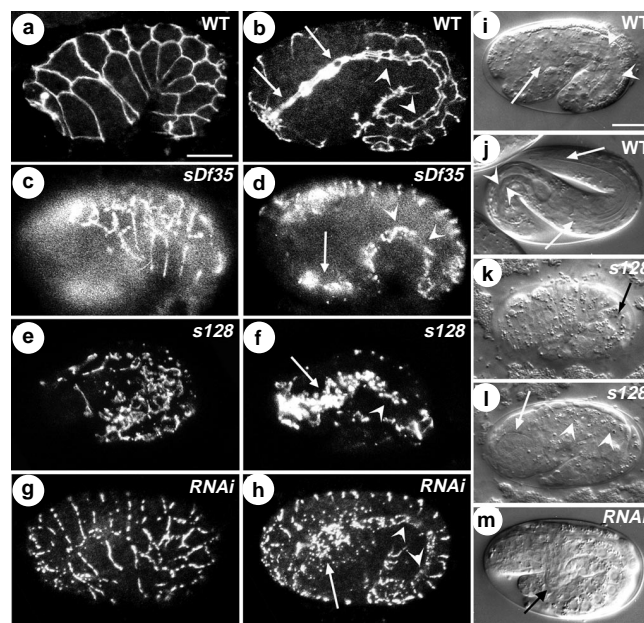
Figure 1 ***let-413* mutants present morphogenetic defects and epithelial abnormalities. a–h**, Immunostaining with the monoclonal antibody MH27, which recognizes adherens junctions in the epidermis, the pharynx (arrows) and the intestine (arrowheads). **i–m**, Nomarski interference microscopy of similar embryos. **a, c, e, g, k**, External focal plane showing the epidermis; **b, d, f, h, l**, internal focal plane of the same embryos showing the pharynx and the intestine; **i, j, m**, internal focal planes. Wild-type 1.5-fold (**a, b, i**) and pretzel (**j**) embryos. **c,d**, *sDf35* homozygous embryo. **e, f, k, l**, Homozygous *let-413 (s128)* embryo. **g, h, m**, *let-413 (RNAi)* embryo (in this and subsequent figures *let-413 (RNAi)* embryo will refer to an embryo laid by a mother in which *let-413* dsRNA had been injected). In mutant embryos, adherens junctions staining is punctate and irregular or absent. In **k** the black arrow points to a large vacuole in the epidermis. In **m**, the ventral epidermis has ruptured and, because of internal pressure, internal cells are leaking out (black arrow). Mutant embryos were collected at 7h development (**g, h**), which is the stage of control embryos in **a, b**, at about 9h development (**c–f, m**), by which time wild-type embryos reach the three-fold stage, or at the end of embryogenesis (15h development; **k, l**). In all pictures anterior is left, dorsal up. Scale bar is10μm.
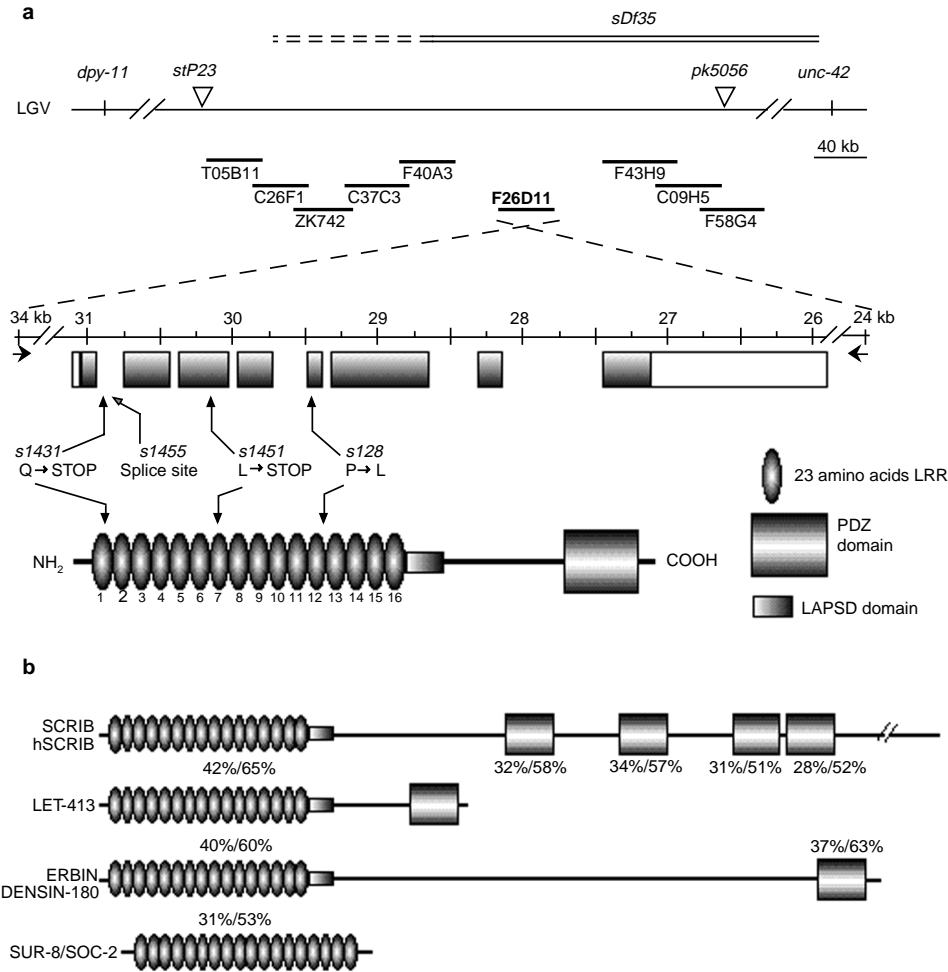
Figure 2 *let-413* encodes a member of the newly defined LAP family of proteins. a, The line LGV represents a portion of the chromosome V genetic map. *stP23* and *pk5056* are transposon insertions used as polymorphisms for mapping. The double line above represents the chromosomal deficiency *sDf35* whose end is not precisely known (dashed lines). Bars below represent cosmids covering the interval, which have been assayed for rescue of *let-413* mutants. Only F26 D11 was able to rescue the *let-413* phenotype. The genomic structure of the *let-413* gene is shown under the scale bar. Grey boxes correspond to coding exons, white boxes to 5′ and 3′ untranslated regions (UTR). Note that exon 5 is 114 nucleotides shorter than the previous prediction in ACeDB. Horizontal arrows show the localization of primers used to generate a long-range PCR product that was shown to rescue the phenotype of *let-413* embryos. The positions of mutations with respect to the gene and the protein sequences are indicated with long arrows, namely *s1431* (30903; C to T), *s1455* (30877; G to A), *s1451* (30184; AATT to TATC) and *s128* (29510; G to A). **b**, Schematic structure of LAP (LRR and PDZ) proteins (see Fig. 3 for further details). The drawings show only ERBIN and SCRIB; DENSIN-180 and hSCRIB have a very similar organization with slight variations in the length of interdomains. Percentages represent identity and similarity of LRR and PDZ of SCRIB and ERBIN compared with LET-413. The LRR domain of LAP proteins is very similar to that of the Ras-binding protein SUR-8/SOC-2.

sheets of epidermal cells spread ventrally and attach to each other at the ventral midline[14]. Elongation is the process by which the embryo achieves its final worm shape and depends on the contraction of actin filaments within epidermal cells[15,16]. Another adherens junction component, as revealed by immunogold electron microscopy (D. Hall, personal communication), is the protein recognized by the monoclonal antibody MH27 (refs 15, 17, 18). The role of *jam-1*, the gene encoding this protein, has not yet been characterized[19]. Here, we report the function of a new gene, *let-413*, which is essential for the assembly of adherens junctions, and yet is localized at the basolateral membrane of epithelial cells.

Results

***let-413* mutants have epithelial defects.** The main classes of epithelial cells in *C. elegans* embryos are found in the epidermis, the intestine and the pharynx[15,20,21]. We previously performed a deficiency screen using the monoclonal antibody MH27 which was aimed at identifying loci required for embryonic morphogenesis[22]. Among the 90 deficiencies that we examined, embryos homozygous for the deficiency *sDf35* display a unique MH27 phenotype. Normally, adherens junctions, as defined by MH27 staining, form a rectilinear pattern around epidermal cells or around the intestine and pharynx lumen (Fig. 1a, b). In *sDf35* embryos, however, adherens junctions are discontinuous or in many areas completely absent (Fig. 1c, d) and the embryo does not elongate beyond the 1.5-fold stage. For simplicity, we will refer to the different stages of embryogenesis by the apparent shape of the embryo: lima bean (epiboly); comma (end of epiboly); 1.5-fold (beginning of elongation); twofold and threefold (active elongation); pretzel (end of elongation). The timing of these stages is given in the legends.

In order to determine if a mutation in a single locus could recapitulate this phenotype, we examined the MH27 staining pattern of embryonic lethal mutations that had previously been isolated and
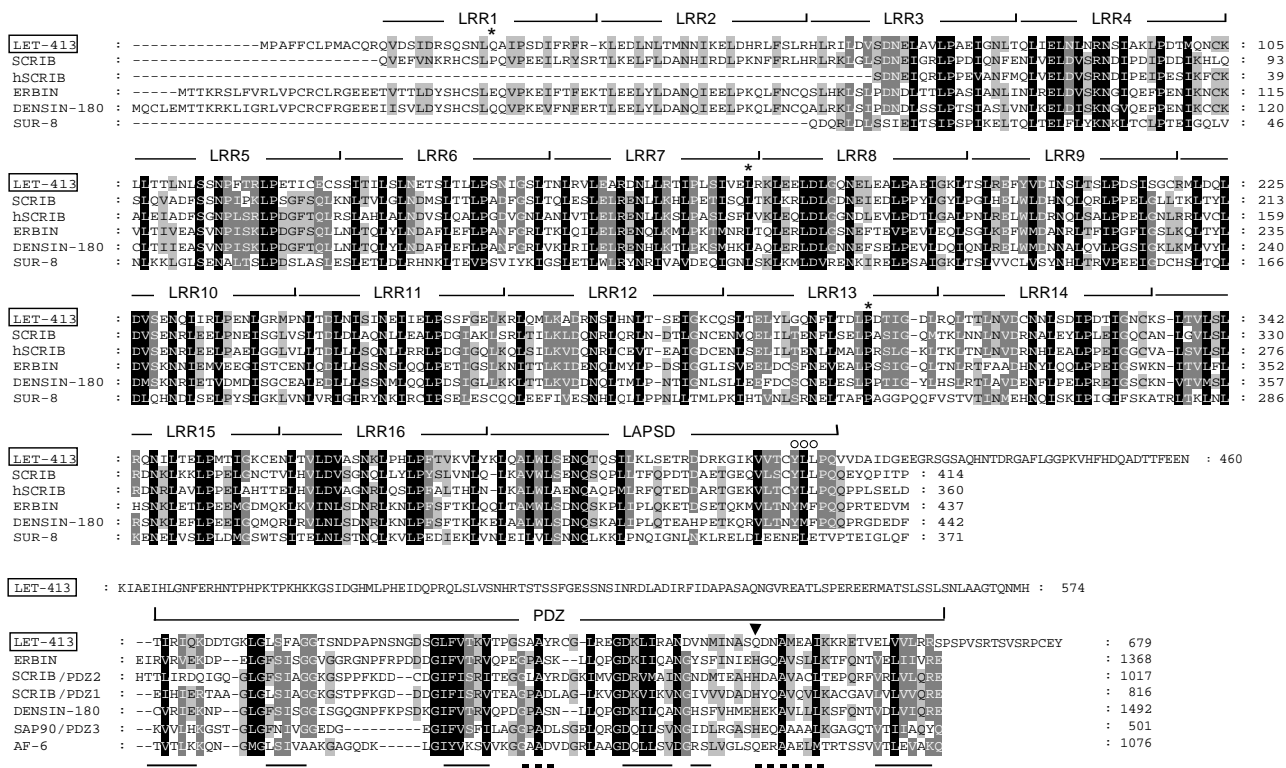
Figure 3 **Alignment of LAP proteins.** Alignments and domain boundaries were obtained with ClustalX[50], using the BLOSUM 35 matrix, and Pfam programme[27]. The complete sequence of LET-413 is shown aligned to the LRR and PDZ domains of other proteins (SUR-8 is also known as SOC-2). The sequence of SCRIB, ERBIN and DENSIN-180 start at the first residue, that of hSCRIB at the first known residue, that of SUR-8/SOC-2 at residue 73. LRR, LAPSD and PDZ domains are indicated with a line; the LAPSD is a new conserved domain with partial homology with two LRR repeats of SUR-8/SOC-2. The first LRR (LRR1) is predicted only for ERBIN and DENSIN-180. Because of the sequence conservation, we suggest that LET-413 and SCRIB also have 16 LRRs. Note that SUR-8/SOC-2 has 18 LRRs, the first of which aligns with the LRR3 of LET-413. The three small open circles above the carboxy terminus of the LAPSD domain indicate a putative basolateral-targeting determinant (see text). SAP90 is an isoform of the PSD-95 MAGUK protein and the first match in blast searches. For simplicity we do not show the PDZ domains of hSCRIB. Dashed and double lines under the PDZ alignments indicate α-helix and β-strands in the structure of the PDZ3 domain of PSD-95. The third β-strand and α-helix are critical for binding specificity[34]. Note that LET-413 has a glutamine residue at the beginning of the α-helix instead of a histidine residue (arrowhead). AF-6 has a group II PDZ domain whereas other PDZ domains are related to group I PDZ domains. Asterisks indicate the position of let-413 mutations. Accession numbers are: SCRIB, AJ252084; hSCRIB, D63481; DENSIN-180, U66707; SUR-8/SOC-2, AF068919; SAP90, AAB48562; AF-6, P55196; the ERBIN sequence was kindly provided by J. P. Borg.

mapped to the area under *sDf35* but had never been characterized[23]. We found that all embryos homozygous for any of the four mutations affecting the gene *let-413* show the same punctate and irregular MH27 staining as *sDf35* embryos (Fig. 1e, f). From the earliest stage of expression, the MH27 pattern in the epidermis, the pharynx and the intestine was abnormal (see Fig. 1g–h for an intermediate stage, and data not shown). By the time control embryos reach the three-fold stage, most *let-413* homozygous embryos had several areas of the epidermis lacking MH27 staining (Fig. 1e). Analysis by Nomarski microscopy showed that all four homozygous *let-413* mutants could not elongate beyond the 1.5-fold/twofold stage (Fig. 1k, l). Upon reaching that stage, about 50% of *let-413* embryos ruptured, often from the ventral side (Fig. 1m), indicating that in *let-413* mutants ventral epidermal cells do not adhere properly to each other after ventral enclosure[14]. Those that did not rupture had vacuoles in their epidermis and loosely adherent epidermal cells, resulting in leakage of internal cells (Fig. 1k). In addition, the pharynx failed to elongate and undergo morphogenesis; similarly the intestine had no discernible lumen and presented some vacuoles (Fig. 1l). In contrast, muscle cells were apparently functional as embryos could twitch. Thus, the results from MH27 staining and Nomarski microscopy are consistent with *let-413* affecting all epithelial cells of the embryo.

let-413 encodes a protein with LRR and PDZ domains. We cloned the *let-413* gene by positional cloning strategies, using genetic mapping, phenotypic rescue experiments and RNA interference[24] (for details see Methods). As described in Fig. 2, we found that a genomic fragment encompassing the putative gene *F26D11.11* is sufficient to rescue *let-413 (s128)*. Moreover, RNA interference directed against *F26D11.11* fully phenocopied the phenotype of *let-413* homozygous embryos in strength and penetrance (Fig. 1g, h, m). Finally, we identified a single change in the *F26D11.11* sequence in each of the four *let-413* alleles, thereby confirming that *F26D11.11* corresponds to *let-413* (Fig. 2a). Specifically, the mutations *s1431* and *s1451* correspond to premature stop codons, *s1455* affects the exon one splice donor and *s128* is a missense mutation converting an invariant proline residue (Fig. 3) into leucine. The nature of *let-413* mutations and the fact that they had similar phenotypes suggest that they are all null or very strong loss of function mutations.

Sequence analysis of two *let-413* cDNAs revealed that they encode a protein of 679 amino acids. Searches in protein databases showed that LET-413 has strong similarity to human ERBIN (J. P. Borg, personal communication), rat DENSIN-180 (ref. 25), and two recently described proteins, *Drosophila* SCRIB[26] and its human
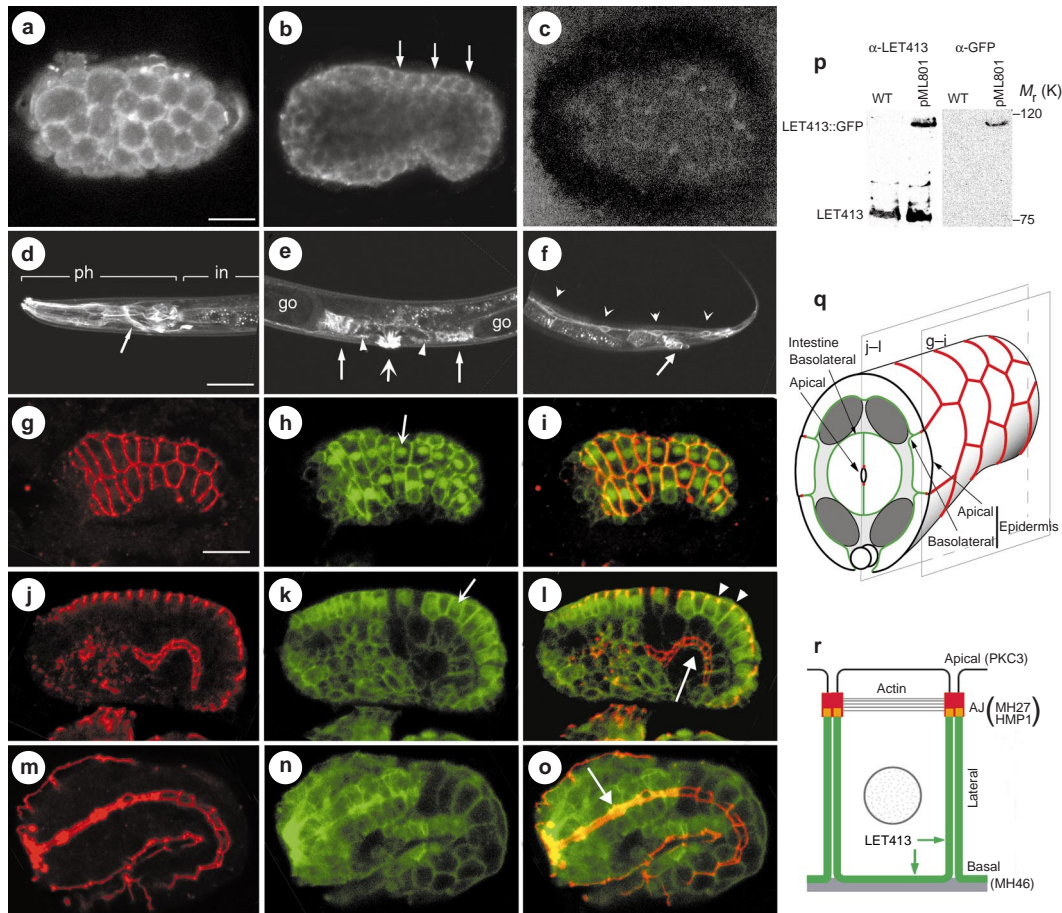
Figure 4 **LET-413 is localized at the basolateral membrane of epithelial cells. a–c**, Immunostaining with an antiserum directed against LET-413. **a**, Early wild-type embryo (2-h/50-cell embryo); at this stage LET-413 is localized uniformly around all cells. **b**, Young comma embryo, internal focal plane; note the membrane staining in epidermal cells (arrows). **c**, *let-413 (RNAi)* comma embryo; staining is abolished showing the specificity of the antiserum. **d–f**, GFP fluorescence of a young *let-413::gfp* transgenic adult, showing the anterior (**d**), mid-body (**e**) and posterior regions (**f**); note the expression in the pharynx (ph), the intestine (in), the nerve ring (arrow in **d**), the vulva (large arrow in **e**), the uterus (arrowheads in **e**), the spermatheca (long arrows in **e**), the rectum (long arrow in **f**) and the lateral epidermis (arrowheads in **f**). Expression in the intestine, which is partially hidden by the gonads (go in **e**), is weaker than in other epithelial tissues. **g–o**, Confocal imaging of *let-413::gfp* embryos after immunostaining with MH27 (**g, j, m**), anti-GFP (membranes) and anti-LIN26 (**h, k, n**; LIN-26 is a nuclear protein in epidermal cells, see arrow in **h** and **k**); merged images are shown in **i**, **l** and **o**. External (**g–i**),and internal (**j–l**) focal planes of a lima bean stage embryo; for a schematic 3D view of the embryo see **q**. **m–o**, Internal focal plane of a twofold stage embryo. The LET-413–GFP signal is partially co-localized with MH27 at the level of adherens junction in the epidermis (arrowheads in **l**) and the pharynx (arrow in **o**). In the intestine (arrow in **l**), the level of expression of LET-413 is too low to detect co-localization with MH27. **p**, Western blot of total protein extract from wild-type and *let-413::gfp* transgenic strains (pML801). The two lanes on the left were probed with LET-413 antiserum, whereas the two lanes on the right were probed with anti-GFP antibodies. The predicted LET-413 relative molecular mass is 75,000 (75 K). Schematic representation of (**q**) the posterior part of a lima-bean embryo (adapted from ref. 15), and (**r**) of a representative epithelial cell. Red represents MH27, green LET-413. The focal planes shown in **g–i** and **j–l** are indicated by open squares. The orange zone (**r**) symbolizes the overlap between MH27 and LET-413–GFP staining domains at the level of adherens junction (AJ), the extent of which is not known owing to technical limitations. PKC-3 is an apical marker expressed in the pharynx and the intestine; the monoclonal antibody MH46 specifically stains the basal membrane of epidermis (see Fig. 5). Scale bar is 10μm, except in **d–f**, where it is 50μm.

ortholgue hSCRIB (Fig. 2b, 3; see Discussion). Further comparison of these proteins using the Pfam protein family database[27] revealed a modular structure consisting of 16 leucine-rich repeats (LRR) of 23 amino acids each and one PDZ domain (LET-413, ERBIN, DENSIN-180) or four (SCRIB, hSCRIB). A new motif (see below) and a variable non-conserved region (Fig. 3) separate these domains. We suggest that LET-413, DENSIN-180, ERBIN, hSCRIB and SCRIB define a new protein family, which we propose to name the LAP family (after LRR and PDZ; proteins with one and four PDZ domain(s) could be further referred to as LAP1 and LAP4 proteins, respectively). Leucine-rich repeats are sequence motifs of 22–29 amino acids, which can be repeated up to 30 times, resulting in a horseshoe-like structure[28,29]. They are believed to mediate protein-protein interactions and are found in proteins with diverse cellular

locations and functions[30]. Interestingly, the *C. elegans* SUR-8/SOC-2 (refs 31, 32), a protein with 18 LRRs according to Pfam, shows 30% amino-acid identity and 53% similarity with the LRR domain of LAP proteins (Fig. 2b, 3). *sur-8* was identified as a suppressor of a dominant activated-Ras mutation and SUR-8 was shown to bind LET-60/Ras through its LRR domain[31], raising the possibility that LAP proteins might also bind small G proteins.

The LRR domain of LAP proteins is followed by a short conserved region of 39 amino acids, which we will refer to as the LAP-specific domain (or LAPSD). The LAPSD shows similarity to a canonical LRR over its first 16 amino acids (Fig. 3). Other LRR-containing proteins often have a short conserved domain following their LRRs[29,30], but the LAPSD domain does not resemble any of these. DENSIN-180, the only LAP protein described so far, was

Figure 5 **The apical compartment and the cytoskeleton are disturbed in epithelia of *let-413* mutants. a–l**, Confocal imaging after immunostaining with MH27 (**a, c**) and anti-GFP antibodies (**b, d** in the same focal plane as in **a, c**), anti PKC-3 antibody (**e, f**), the mAb MH46 (**g, h**) or after rhodamine-conjugated phalloidin staining (**i–l**). **a–d**, Strain carrying an integrated *hmp-1*::*gfp* marker. **a, b**, External view of a 1.5-fold control embryo; most of HMP-1–GFP is membrane-bound and co-localizes with MH27 in epidermal cells (arrows). **c, d**, External view of a 1.5-fold *let-413 (RNAi)* embryo; HMP-1–GFP is almost entirely cytoplasmic. **e, g**, Wild-type 1.8-fold embryo. **f, h**, 1.5-fold *let-413 (RNAi)* embryo. In *let-413* embryos, apical marker of the pharynx and the intestine is completely absent or mislocalized, whereas epidermal basal attachments are correctly organized although slightly larger than in the wild-type embryos. Insets in **e** and **f** correspond to the merge pictures (red MH27, green anti-PKC-3) of the regions indicated by the white rectangle. **i, k**, Wild-type embryos: 1.5-fold stage, external view (**i**) and two-fold stage, internal view (**k**). **j, l**, *let-413 (RNAi)* embryos: 1.5-fold stage, external view (**j**); two-fold stage, internal view (**l**). Note the thin and regularly spaced actin filaments in wild-type embryos (arrowheads in **i**) and the thick and disorganized actin bundles in *let-413* mutants (arrows in **j**). Pharyngeal and intestinal actin filaments (long and short arrows in **k–l**) are also very abnormal; the oblique arrow points to the nerve ring (**k–l**). Scale bar is 10 μm.

purified from postsynaptic density fractions[25]. It has been suggested that DENSIN-180 might contain a transmembrane domain and could act as an adhesion molecule. We did not find any evidence of a transmembrane domain or of a peptide signal in LET-413, but noticed that some of the conserved residues within the carboxy terminus of the LAPSD correspond to a tyrosine or a dileucine followed by acidic residues. Both motifs have been proposed to be basolateral-targeting determinants[33], which might be relevant given the localization of LET-413 (see below). PDZ domains have been classified into two major groups on the basis of sequence similarities and on their binding specificity[34]. The PDZ domain(s) of LAP proteins are most similar to group I PDZ domains (Fig. 3); however, LET-413 lacks a key histidine residue that is thought to be important for binding specificity, suggesting that is might not bind the same targets as other LAP proteins. In summary, the structure of LET-413 suggests that it might interact with different sets of proteins through its LRR and PDZ domains.

LET-413 is a basolateral membrane protein in epithelial cells. To determine the expression pattern and subcellular localization of LET-413, we raised an anti-peptide antiserum that recognized a band of the expected size in western blots (Fig. 4p). In addition, we constructed a translational fusion between *let-413* and a cDNA coding for green fluorescent protein (GFP)[35] that was inserted just prior to the stop codon of *let-413*. Injection of this *let-413::gfp* construct fully rescued the phenotype of *let-413(s128)* mutants, indicating that LET-413–GFP is functional. This construct, which gave a bright signal in transgenic animals, was used to identify cells expressing *let-413*.

Using antibodies and the GFP-reporter construct we found that LET-413 is always associated with membranes. In early embryos and until the lima bean stage, LET-413 was ubiquitously expressed (Fig. 4a). As development proceeds, expression became restricted to epithelial cells, and was stronger in the epidermis and the pharynx than in the intestine (Fig. 4b, h, k, n). Throughout larval develop-

ment and in adults LET-413–GFP was detected in epidermal seam cells, the pharynx, the rectum, the excretory pore, and more weakly in the intestine (Fig. 4d–f). Expression was also detected in epithelial tissues contributing to the reproductive system, namely the vulva, the uterus and the spermatheca (Fig. 4e). In addition to this epithelial expression, LET-413 was detected in the nerve ring (Fig. 4d). To determine the precise localization of LET-413, we performed confocal analysis on *let-413::gfp* transgenic embryos using MH27 to visualize adherens junctions (Fig. 4g–o; for a spatial view of the embryo, see Fig. 4q). We found that LET-413–GFP was uniformly localized along the basolateral membrane (Fig. 4k, and schematically shown in Fig. 4r), but was not detected in the apical membrane in any epithelial tissue. Within the limits of resolution of confocal microscopy, the apical-most boundary of the LET-413 expression domain in the epidermis and the pharynx appeared to partially overlap with adherens junctions (Fig. 4i, l, o). In conclusion, LET-413 is associated with the basolateral membrane of epithelial cells.

Apical and cytoskeletal defects in *let-413* mutants. To determine whether the MH27 staining defects observed in *let-413* mutants reflect a general disorganization of epithelial cells, we examined the localization of several markers located in different cell compartments. We first examined the distribution of another adherens junction-associated protein, the α-catenin HMP-1 (ref. 13), using a *hmp-1::gfp* construct that can rescue the *hmp-1* phenotype[14]. In control embryos, HMP-1–GFP co-localizes with MH27 in epidermal cells (Fig. 5a, b). In contrast, in 25 out of 47 *let-413* mutant embryos that we examined, HMP-1–GFP appeared to be essentially cytoplasmic instead of membrane bound (Fig. 5c, d). In the remaining 22 mutant embryos some membrane-bound HMP-1–GFP was present in certain epithelial cells, but it was less abundant than in control embryos (data not shown). We also examined the distribution of the only available apical marker, the atypical protein kinase PKC-3 (ref. 36), which is localized at the apical membrane of pharyngeal and intestinal epithelial cells[21] (Fig. 5e). In *let-413* mutants,

Figure 6 **Adherens junctions are abnormal and mislocalized in let-413 embryos.** Electron microscopy analysis of adherens junctions (arrowheads) in the intestine (**a–d**) and epidermis (**e–h**) of wild-type (**a**, **e**) and *let-413 (RNAi)* (**b–d**, **f–h**) embryos. Inset in **a** corresponds to a higher magnification of the region indicated by a white arrow. In *let-413* embryos, adherens junctions were extended (**b**, **h**), interrupted (**c**, **f**, **h**) or essentially absent (**d**, **g**); magnifications in **b–d** are the same as for the inset in **a**; thus the sizes of junctions are directly comparable. Long open arrows (**f**, **h**) point to an abnormally large space between the membranes of neighbouring epidermal cells; black arrows (**g**, **h**) point to long overlapping extensions of the apical part of epidermal cells. N, nucleus; Y, yolk droplets; L, lipid droplet. Scale bar is 300 nm.

a reduction in its diameter and consequent antero-posterior elongation[15]. As *let-413* embryos do not elongate beyond the 1.5-or twofold stage and adherens junctions appear disorganized, we examined the actin cytoskeleton by staining with rhodamine-conjugated phalloidin. We found that actin filaments in the epidermis of *let-413(RNAi)* embryos formed large and irregularly spaced bundles (compare Fig. 5j, i). These bundles might arise from the attachment of actin to discrete areas of the apico-lateral membrane where some MH27 staining is still visible. In the pharynx and the intestine, the actin cytoskeleton was also clearly abnormal (Fig. 5l). Similar defects were observed in *let-413 (s128)* mutant embryos (data not shown). We do not think that the adherens junction defects described so far could result from cytoskeletal abnormalities, as *hmp-1*, *hmp-2* and *hmr-1* mutants cause much more severe cytoskeletal defects without affecting adherens junctions[13]. In conclusion, we found that basally located attachments are normal, in contrast to apical and adherens junctions markers which were disrupted in *let-413* embryos.

Severe adherens junction structural defects in *let-413* mutants. To examine the structure of junctions in *let-413* mutants we performed electron microscopy analysis. In wild type embryos, adherens junctions in the intestine (Fig. 6a) and the epidermis (Fig. 6e) are precisely defined and localized in close proximity to the apical membrane. In contrast in *let-413* embryos, extended but generally discontinuous electron dense structures reminiscent of adherens junctions were observed (Fig. 6b, c, f, h). In some cases, these structures were very small or could hardly be detected (Fig. 6d, g). In the intestine these adherens-like junctions remained close to the lumen as in wild-type embryos (Fig. 6b, c), whereas in the epidermis they were observed along the lateral membrane (Fig. 6f, h). At some places, the membranes of neighbouring cells were not apposed and the extracellular space appeared larger (Fig. 6f, h). Absence of properly positioned junctions caused apical regions of epidermal cells to overlap and interdigitate (Fig. 6g, h). We did not examine in details the structure of adherens junctions in the pharynx. These data clearly show that *let-413* is required for the proper organization and positioning of adherens junctions.

Discussion

We have characterized the gene *let-413* in *C. elegans*, which defines a new protein family that combines an LRR domain, likely to interact with small GTPases, with a PDZ domain related to the PDZ domains of MAGUK proteins. A striking feature of *let-413* mutants is that the most severely affected structures are located apically, whereas the LET-413 protein is located at the basolateral membrane.

Our analysis revealed that epithelial integrity is severely affected in *let-413* mutants, leading to abnormal morphogenesis of the pharynx, intestine and embryo. At the ultrastructural level, we found either that adherens junctions are missing or that discontinuous junction-like structures are located at more basolateral positions. Consistent with the absence of normal junctions, the apical edge of the epidermal cells shows a marked disorganization. At the molecular level, we found in *let-413* mutants that two adherens junction markers, the protein recognized by the monoclonal antibody MH27 (JAM-1) and the α-catenin homologue HMP-1 (refs 14, 15, 17 and D. Hall, personal communication), were missing in many areas. In parallel, we observed that the atypical protein kinase C PKC-3 is essentially absent from the intestinal and pharyngeal apical membranes. These data suggest that some aspects of epithelial cell polarity are severely compromised in *let-413* mutant embryos. As LET-413 is located basolaterally, we suggest that apical abnormalities do not result directly from absence of the protein but are more likely to result from the absence of normal junctions. As far as we could tell (Fig. 1 and data not shown), JAM-1 was not located at lateral positions corresponding to those at which we observed electron-dense structures, suggesting that those adherens-like junctions may not always contain the JAM-1 protein. One pos-

staining with anti-PKC-3 antibodies was barely detectable and punctate (Fig. 5f). In contrast, we found that the distribution of three basal markers was not affected in the epidermis of *let-413* embryos. Specifically, we used three monoclonal antibodies that recognize two components of epidermal hemidesmosomes (MH4, MH5)[17], and a transmembrane protein located at the basal side of epidermal cells that spans the basement membrane to anchor muscle cells to epidermal cells (MH46)[37]. The basal markers recognized by these antibodies proved to be similarly located at the muscle/epidermis interface in wild-type and mutant embryos, although their organization was slightly more irregular in *let-413* mutants (Fig. 5g, h; and data not shown). Consistent with this observation, we found using a muscle marker that muscle cells are correctly organized (data not shown).

During *C. elegans* morphogenesis, actin filaments within epidermal cells contract along the circumference of the embryo leading to

sibility is that JAM-1 is degraded or not properly inserted in the membrane when junctions are mispositioned. Despite their mislocalization, lateral adherens-like junctions might initially maintain the cohesion of the epidermis, as *let-413* mutant embryos could enclose ventrally (although less than 50% of them maintained enclosure) and initiate body elongation.

The phenotype of *let-413* embryos is reminiscent of that observed after *crumbs* overexpression in *Drosophila* embryos[6,38]. These embryos assemble adherens-like junctions at more basolateral positions and have membranes between adjacent epithelial cells that tend to separate, and then present some epithelial cell polarity defects. It has been proposed that the proteins Crumbs and DLT form a scaffold that delimits the apical border where the adherens junctions form[5–7]. By analogy with the DLT/Crumbs system, we suggest that LET-413 and other LAP proteins might provide a scaffold within the basolateral domain to assemble adherens junctions, possibly by defining their basal boundary.

Any model to explain LET-413 function should take into account its modular structure. A salient feature of LET-413 is the presence of an LRR domain strongly homologous to SUR-8/SOC-2, a protein known to bind the G protein Ras[31]. Mutations in LET-60/Ras generally result in cell-fate specification defects[39]. As we did not observe cell-fate defects in *let-413* mutants, we suggest that LAP proteins interact with a GTPase different from Ras. On the basis of LET-413 localization and mutant phenotypes, this GTPase would act at the basolateral membrane by polarizing the cytoskeleton and/or protein trafficking. Among the small GTPase families, the Rho/Rac/Cdc42 and some of the Rab GTPases meet these criteria. Rho/Rac/Cdc42 GTPases have been associated with many processes linked to cell polarity, in particular those that involve the actin cytoskeleton[40]; more recently they have been implicated in polarized secretion and endocytosis[41,42]. Rab proteins are well known for their role in vesicular trafficking[43]. It has recently been proposed that spatial landmarks for vesicle docking within the plasma membrane have an essential role during development of epithelial cells to reinforce and maintain the delivery of proteins that are constitutively sorted in the Golgi[1]. We suggest that many features characterizing *let-413* qualify this gene for acting as a similar docking platform in a trafficking pathway controlled by one of the GTPases mentioned above. Part of its trafficking function would be to assist in the assembly of adherens junctions.

While this work was being reviewed, it was shown that mutations affecting the *Drosophila* gene *scribble*, which is identical to *vartul* (see Fig. 3), display very similar characteristics to *let-413* mutants[26]. We believe that LAP proteins define a new evolutionarily conserved signal transduction pathway that impacts on the development of epithelial cells. Further analyses in *C. elegans* should undoubtedly prove useful in unravelling this pathway.

Note added in proof: For a description of the ERBIN protein, see the accompanying article by Borg *et al.*, p407. □

Methods

Strains and genetics.
Animals were propagated and genetic analyses were performed as described[44]. The following mutations and markers were used: *dpy-11 (e224)* V; *unc-42 (e270)* V; *rol-3 (e754)* V; *sDf35* V; *jcIs1 [unc-29 (+)-rol-6 (su1006)-jam1::gfp][19,44,45]*. The strain carrying *svIs13 [dpy-20 (+)-hmp-1::gfp]* was a kind gift from S. Tuck. The *let-413* mutations *s128, s1431, s1451* and *s1455* were generated by ethyl methyl sulphonate (EMS) mutagenesis of the Bristol strain N2 in a saturation screen for lethal mutations[23]. Initial mapping placed *s1431* and *s1451* between *dpy-11* and *unc-42* and under the deficiency *sDf35*, which they failed to complement. Three-factor mapping positioned *let-413* between *stP23* and *pk5056*, which correspond to Tc1 transposons present in the Bergerac background (strains RW7000 and NL7000, respectively; see the database ACeDB and references therein) but absent from N2. From *dpy-11(e224) +let-413(s128) unc-42 (e270)/+ stP23 + +* heterozygotes, 15/15 Unc non-Let and 19/22 Dpy non-Let recombinants had *stP23*; from *dpy-11 (e224) let-413 (s128) + unc-42 (e270)/+ + pk5056 +* heterozygotes, 31/33 Unc non-Let and 60/60 Dpy recombinants had *pk5056*.

Molecular biology.
The interval defined by *stP23* and *pk5056* is 400 kilobases (kb) long and is covered by a contig containing two cosmid gaps of about 40 kb each. To identify *let-413*, we used cosmid rescue and RNA interference to see if interference with any predicted genes in the interval would phenocopy the *let-413* phenotype.

The templates used for RNA synthesis were amplified by PCR using primers that were derived from the genomic sequence of the *let-413* area and carried a T3 promoter sequence at their 5′ end (ATTAACCCTCACTAAAGG). DsRNA was microinjected into the syncytial gonad arms of N2 and *jam1::gfp* animals. Cosmid F26 D11 (EMBL accession number AF068716) was found to fully rescue *let-413 (s128)* animals, whereas other cosmids did not. Note that the cosmid F26 D11 is mispositioned on the physical map of the latest available version of ACeDB. In order to identify *let-413* mutations, each exon and flanking splice sites were amplified from unhatched *let-413* embryos[46] and sequenced from three independent amplifications. Transgenic lines were established using plasmids pPD93, 97 (*myo3::gfp*)[24] or pRF4 (*rol-6 (su1006)*)[47] as co-injection markers. Rescue was assayed by injecting cosmids or long-range PCR fragments into *let-413 (s128) unc-42 (e270)V/rol3 (e754)* animals. The sequences of the cDNAs *yk660h2* and *yk126a10* isolated by Y. Kohara were established and compared with the genomic sequence[48]. Reverse transcription polymerase chain reaction (RT-PCR) experiments indicated that *let-413* transcripts are *trans*-spliced to SL1 (data not shown). Plasmid pML801 is a *let-413::gfp* translational fusion obtained by cloning the complete *let-413* coding sequence and a 3-kb upstream sequence (positions 34,000 to 25, 110 in F26 D11) between the *Bam*HI and *Asp* 718 sites of pPD95.75 (a kind gift from A. Fire).

Antibodies and staining.
A peptide of 19 amino acids ((C)GGTSNDPAPNSNGDS; single-letter amino-acid notation) was conjugated to ovalbumin and used to generate rabbit polyclonal antibodies. Immunocytochemistry was performed as described[22,49]. Phalloidin staining was performed as described elsewhere[13]. Pictures were captured on a Leica TCS3 D confocal microscope. Protein extracts and western blotting were carried out as described[49].

Electron microscopy.
Embryos were mounted on agarose pads containing 4% glutaraldehyde, and the eggshell was broken with a laser beam according to a protocol suggested by D. Hall (see http://www.aecom.yu.edu/wormem). Only embryos that had reached the 1.5-fold to 1.7-fold stage and that had not ruptured were processed. Subsequently, embryos were fixed overnight on the agar pad, and post-fixed with osmium tetroxide and uranyl acetate as described elsewhere[49]. Plastic sections of 70 nm were contrasted with uranyl acetate and lead citrate and observed with a Philips EM208 microscope, operating at 80 kV.

1. Yeaman, C., Grindstaff, K. K. & Nelson, W. J. New perspectives on mechanisms involved in generating epithelial cell polarity. *Physiol. Rev.* **79**, 73–98 (1999).
2. Baumgartner, S. *et al.* A *Drosophila* neurexin is required for septate junction and blood-nerve barrier formation and function. *Cell* **87**, 1059–1068 (1996).
3. Woods, D. F., Hough, C., Peel, D., Callaini, G. & Bryant, P. J. Dlg protein is required for junction structure, cell polarity, and proliferation control in *Drosophila* epithelia. *J. Cell Biol.* **134**, 1469–1482 (1996).
4. Ward, R. E., Lamb, R. S. & Fehon, R. G. A conserved functional domain of *Drosophila* coracle is required for localization at the septate junction and has membrane-organizing activity. *J. Cell Biol.* **140**, 1463–1473 (1998).
5. Bhat, M.A. *et al.* Discs Lost, a novel multi-PDZ domain protein, establishes and maintains epithelial polarity. *Cell* **96**, 833–845 (1999).
6. Klebes, A. & Knust, E. A conserved motif in Crumbs is required for E-cadherin localisation and zonula adherens formation in *Drosophila*. *Curr. Biol.* **10**, 76–85 (2000).
7. Yeaman, C., Grindstaff, K.K., Hansen, M.D. & Nelson, W.J. Cell polarity: Versatile scaffolds keep things in place. *Curr. Biol.* **9**, R515–517 (1999).
8. Tepass, U., Theres, C. & Knust, E. *crumbs* encodes an EGF-like protein expressed on apical membranes of *Drosophila* epithelial cells and required for organization of epithelia. *Cell* **61**, 787–799 (1990).
9. Ponting, C.P., Phillips, C., Davies, K.E. & Blake, D.J. PDZ domains: targeting signalling molecules to sub-membranous sites. *BioEssays* **19**, 469–479 (1997).
10. Hoskins, R., Hajnal, A.F., Harp, S.A. & Kim, S.K. The *C. elegans* vulval induction gene *lin-2* encodes a member of the MAGUK family of cell junction proteins. *Development* **122**, 97–111 (1996).
11. Simske, J. S., Kaech, S. M., Harp, S. A. & Kim, S. K. LET-23 receptor localization by the cell junction protein LIN-7 during *C. elegans* vulval induction. *Cell* **85**, 195–204 (1996).
12. Kaech, S.M., Whitfield, C. W. & Kim, S.K. The LIN-2/LIN-7/LIN-10 complex mediates basolateral membrane localization of the *C. elegans* EGF receptor LET-23 in vulval epithelial cells. *Cell* **94**, 761–771 (1998).
13. Costa, M. *et al.* A putative catenin-cadherin system mediates morphogenesis of the *Caenorhabditis elegans* embryo. *J. Cell Biol.* **141**, 297–308 (1998).
14. Raich, W. B., Agbunag, C. & Hardin, J. Rapid epithelial-sheet sealing in the *Caenorhabditis elegans* embryo requires cadherin-dependent filopodial priming. *Curr. Biol.* **9**, 1139–1146 (1999).
15. Priess, J. R. & Hirsh, D. I. *Caenorhabditis elegans* morphogenesis: the role of the cytoskeleton in elongation of the embryo. *Dev. Biol.* **117**, 156–173 (1986).
16. Wissmann, A., Ingles, J., McGhee, J. D. & Mains, P. E. *Caenorhabditis elegans* LET-502 is related to Rho-binding kinases and human myotonic dystrophy kinase and interacts genetically with a homolog of the regulatory subunit of smooth muscle myosin phosphatase to affect cell shape. *Genes Dev.* **11**, 409–422 (1997).
17. Francis, R. & Waterston, R. H. Muscle cell attachment in *Caenorhabditis elegans*. *J. Cell Biol.* **114**, 465–479 (1991).
18. Podbilewicz, B. & White, J. G. Cell fusions in the developing epithelial of *C. elegans*. *Dev. Biol.* **161**, 408–424 (1994).
19. Mohler, W. A., Simske, J. S., Williams-Masson, E. M., Hardin, J. D. & White, J. G. Dynamics and ultrastructure of developmental cell fusions in the *Caenorhabditis elegans* hypodermis. *Curr. Biol.* **8**, 1087–1090 (1998).
20. White, J. In *The Nematode Caenorhabditis elegans* (ed. Wood, W. W. and the Community of *C. elegans* Researchers) 81–122 (Cold Spring Harbor Laboratory Press, Cold Spring Harbor, New York, 1988).
21. Leung, B., Hermann, G. J. & Priess, J. R. Organogenesis of the *Caenorhabditis elegans* intestine. *Dev.*

Biol. **216**, 114–134 (1999).

22. Labouesse, M. Deficiency screen based on the monoclonal antibody MH27 to identify genetic loci required for morphogenesis of the *Caenorhabditis elegans* embryo. *Dev. Dyn.* **210**, 19–32 (1997).

23. Johnsen, R. C. & Baillie, D. L. Genetic analysis of a major segment [LGV(left)] of the genome of *Caenorhabditis elegans. Genetics* **129**, 735–752 (1991).

24. Fire, A. *et al.* Potent and specific genetic interference by double-stranded RNA in *Caenorhabditis elegans. Nature* **391**, 806–811 (1998).

25. Apperson, M. L., Moon, I. S. & Kennedy, M. B. Characterization of densin-180, a new brain-specific synaptic protein of the O-sialoglycoprotein family. *J. Neurosci.* **16**, 6839–6852 (1996).

26. Bilder, D. & Perrimon, N. Localization of apical epithelial determinants by the basolateral PDZ protein Scribble. *Nature* **403**, 676–680 (2000).

27. Bateman, A. *et al.* The Pfam Protein Families Database. *Nucleic Acids Res.* **28**, 263–266 (2000).

28. Kobe, B. & Deisenhofer, J. Crystal structure of porcine ribonuclease inhibitor, a protein with leucine-rich repeats. *Nature* **366**, 751–756 (1993).

29. Hillig, R. C. *et al.* The crystal structure of rna1 p: a new fold for a GTPase-activating protein. *Mol. Cell* **3**, 781–791 (1999).

30. Kajava, A. V. Structural diversity of leucine-rich repeat proteins. *J. Mol. Biol.* **277**, 519–527 (1998).

31. Sieburth, D. S., Sun, Q. & Han, M. SUR-8, a conserved Ras-binding protein with leucine-rich repeats, positively regulates Ras-mediated signaling in *C. elegans. Cell* **94**, 119–130 (1998).

32. Selfors, L. M., Schutzman, J. L., Borland, C. Z. & Stern, M. J. soc-2 encodes a leucine-rich repeat protein implicated in fibroblast growth factor receptor signaling. *Proc. Natl Acad. Sci. USA* **95**, 6903–6908 (1998).

33. Matter, K. Epithelial polarity: sorting out the sorters. *Curr. Biol.* **9**, R39-R42 (1999).

34. Songyang, Z. *et al.* Recognition of unique carboxyl-terminal motifs by distinct PDZ domains. *Science* **275**, 73–77 (1997).

35. Chalfie, M., Tu, Y., Euskirchen, G., Ward, W. W. & Prasher, D. C. Green fluorescent protein as a marker for gene expression. *Science* **263**, 802–805 (1994).

36. Tabuse, Y. *et al.* Atypical protein kinase C cooperates with PAR-3 to establish embryonic polarity in *Caenorhabditis elegans. Development* **125**, 3607–3614 (1998).

37. Hresko, M. C., Schriefer, L. A., Shrimankar, P. & Waterston, R. H. Myotactin, a novel hypodermal protein involved in muscle-cell adhesion in *Caenorhabditis elegans. J. Cell Biol.* **146**, 659–672 (1999).

38. Grawe, F., Wodarz, A., Lee, B., Knust, E. & Skaer, H. The *Drosophila* genes *crumbs* and *stardust* are involved in the biogenesis of adherens junctions. *Development* **122**, 951–959 (1996).

39. Sternberg, P. W. & Han, M. Genetics of RAS signaling in *C. elegans. Trends Genet.* **14**, 466–472 (1998).

40. Hall, A. Rho GTPases and the actin cytoskeleton. *Science* **279**, 509–514 (1998).

41. Kroschewski, R., Hall, A. & Mellman, I. Cdc42 controls secretory and endocytic transport to the basolateral plasma membrane of MDCK cells. *Nature Cell Biol.* **1**, 8–13 (1999).

42. Adamo, J. E., Rossi, G. & Brennwald, P. The rho GTPase *rho3* has a direct role in exocytosis that is distinct from its role in actin polarity. *Mol. Biol. Cell* **10**, 4121–4133 (1999).

43. Martinez, O. & Goud, B. Rab proteins. *Biochim. Biophys. Acta* **1404**, 101–112 (1998).

44. Brenner, S. The genetics of *Caenorhabditis elegans. Genetics* **77**, 71–94 (1974).

45. McKim, K. S., Heschl, M. F., Rosenbluth, R. E. & Baillie, D. L. Genetic organization of the *unc-60* region in *Caenorhabditis elegans. Genetics* **118**, 49–59 (1988).

46. Williams, B. D., Schrank, B., Huynh, C., Shownkeen, R. & Waterston, R. H. A genetic mapping system in *Caenorhabditis elegans* based on polymorphic sequence-tagged sites. *Genetics* **131**, 609–624 (1992).

47. Mello, C. & Fire, A. DNA transformation. *Methods Cell Biol.* **48**, 451–482 (1995).

48. The *C. elegans* Sequence Consortium. Genome sequence of the nematode *C. elegans*: A platform for investigating biology. *Science* **282**, 2012–2018 (1998).

49. Labouesse, M., Hartwieg, E. & Horvitz, H. R. The *Caenorhabditis elegans* LIN-26 protein is required to specify and/or maintain all non-neuronal ectodermal cell fates. *Development* **122**, 2579–2588 (1996).

50. Thompson, J. D., Gibson, T. J., Plewniak, F., Jeanmougin, F. & Higgins, D. G. The CLUSTAL_X windows interface: flexible strategies for multiple sequence alignment aided by quality analysis tools. *Nucleic Acids Res.* **25**, 4876–4882 (1997).